

1 **Saline groundwater evolution in Luanhe River Delta, China since**  
2 **Holocene: hydrochemical, isotopic and sedimentary evidence**

3 Xianzhang Dang<sup>a, b, c</sup>, Maosheng Gao<sup>b, d</sup>, Zhang Wen<sup>a</sup>, Guohua Hou<sup>b, d</sup>, Hamza Jakada<sup>e</sup>,  
4 Daniel Ayejoto<sup>a</sup>, Qiming Sun<sup>a, b, c</sup>

5 <sup>a</sup>School of Environmental Studies, China University of Geosciences, 388 Lumo Rd,  
6 Wuhan, 430074, China

7 <sup>b</sup>Qingdao Institute of Marine Geology, CGS, Qingdao, 266071, China

8 <sup>c</sup>Chinese Academy of Geological Sciences, Beijing, 100037, China

9 <sup>d</sup>Laboratory for Marine Geology, Pilot National Laboratory for Marine Science and  
10 Technology, Qingdao, 266071, China

11 <sup>e</sup>Department of Civil Engineering, Baze University Abuja, Nigeria

12 *Correspondence to:* Maosheng Gao (gaomsh66@sohu.com), Zhang Wen  
13 (wenz@cug.edu.cn)

14

1 **Abstract**

2 Since the Quaternary Period, palaeo-seawater intrusions have been suggested to explain  
3 the observed saline groundwater that extends far inland in coastal zones. The Luanhe  
4 River Delta (northwest coast of Bohai Sea, China) is characterized by the distribution  
5 of saline, brine, brackish and fresh groundwater, from coastline to inland, with a wide  
6 range of total dissolved solids (TDS) between 0.38-125.9 g/L. Meanwhile, previous  
7 studies have revealed that this area was significantly affected by Holocene marine  
8 transgression. In this study, we used hydrochemical, isotopic, and sedimentological  
9 methods to investigate groundwater salinization processes in the Luanhe River Delta  
10 and its links to the palaeo-environmental settings. The isotopic results ( $^2\text{H}$ ,  $^{18}\text{O}$ ,  $^{14}\text{C}$ )  
11 facilitate the distinction between old and new groundwater recharge. Results of the  
12 hydro-chemical analysis using PHREEQC indicate that the origin of salt in saline and  
13 brine groundwater is from a marine source. The  $^{18}\text{O}$ -Cl relationship diagram yields  
14 three end-member mixing of groundwater with two mixing scenarios suggested to  
15 explain the freshening and salinization processes in study area. When interpreted with  
16 data from palaeo-environmental sediments, we found that groundwater salinization  
17 may have occurred since the Holocene marine transgression. The brine is characterized  
18 by radiocarbon activities of ~50 to 85 pMC and relatively depleted stable isotopes,  
19 which is associated with seawater evaporation in the ancient lagoon during delta  
20 progradation, as well as mixing with deeper fresh groundwater which probably was  
21 recharged in cold late Pleistocene. As for the brackish and fresh groundwater, they are  
22 characterized by river-like stable isotope values where high radiocarbon activities

1 (74.3 to 105.9 pMC) were formed after the wash-out of salinized aquifer by surface  
2 water in the delta plain. This study presents an approach for utilizing geochemical  
3 indicator analysis with paleogeographic reconstruction to better assess groundwater  
4 evolutionary patterns in coastal aquifers.

5

## 1 **Introduction**

2 It is estimated that 20-40% of the world's population lives in coastal areas. (Small  
3 and Nicholls, 2003; Martinez et al., 2007; UN Atlas, 2010). Groundwater is the primary  
4 source of fresh water in this region (Cary et al., 2015). However, groundwater  
5 salinization poses a significant threat to everyday living and development activities  
6 (Cost Environment Action 621, 2005; de Montety et al., 2008). In recent decades,  
7 groundwater salinization in coastal zones are widely concerned and studied. On the one  
8 hand, seawater intrusion due to groundwater pumping is a vital salinization process in  
9 the coastal aquifer (Reilly and Goodman, 1985; Werner, 2010, 2013; Han and Currell,  
10 2018). On the other hand, groundwater salinization caused by the palaeo-seawater  
11 intrusion, in response to the Quaternary changes in global sea-level, has been reported  
12 in many coastal zones worldwide (Edmunds, 2001; Akouvi, 2008; Santucci et al., 2016,  
13 Larsen et al., 2017).

14 Coastal aquifers are linked to the ocean and continental hydrological cycle (Ferguson  
15 and Gleeson, 2012), both of which are influenced by natural and human-induced change  
16 (Jiao and Post, 2019). There is a steady-state seawater-freshwater interface under the  
17 natural state that extends inland from the coastal line (Costall et al., 2020). Since the  
18 Quaternary period, however, sea-level fluctuations on geological timescales have  
19 caused the interface to change, allowing seawater intrusion during transgression events  
20 and freshwater flushing during glacial low sea-level periods, which are evident in  
21 hydrochemical characteristics of groundwater in coastal aquifers(Kooi et al., 2000;  
22 Sanford, 2010; Aquilina et al., 2015; Lee et al., 2016). In addition, the hypersaline

1 groundwater found in coastal zones, particularly brine groundwater with a salinity of  
2 2-4 times that of seawater, cannot be explained solely by using a seawater intrusion  
3 model (Sola et al., 2014, Han et al., 2020), and palaeoenvironment settings must be  
4 taken into consideration (Van Engelen et al., 2019). Some studies, for example, attribute  
5 the presence of brine in Mediterranean countries to the evaporation of seawater in the  
6 lagoon system during the Holocene transgression (Giambastiani et al., 2013, Vallejos  
7 et al., 2018).

8 The Bohai Sea of northern China was affected by Late Pleistocene transgressive-  
9 regressive cycles, which caused various salinity palaeo-saltwater intrusion along the  
10 coastal aquifers (Du et al., 2015; Li et al., 2017). Several studies have applied  
11 geochemical methods to elucidate the origin of saline groundwater and the salinization  
12 processes under anthropogenic influence, including induced mixing brine water from  
13 adjacent aquifers caused by groundwater overexploitation in Laizhou Bay (Han et al.,  
14 2011, 2014; Liu et al., 2017; Qi et al., 2019). However, the association between  
15 groundwater salinization (especially brine formation) and palaeoenvironmental  
16 implications are still not clear. Thus, this study applies a range of chemical, isotopic  
17 and sedimentary indicators to examine the Luanhe River Delta (situated along the  
18 northwestern coast of Bohai Sea) to elucidate the groundwater salinization processes in  
19 relation to recharge, salt source, mixing behavior and palaeogeographic evolution. The  
20 overall goal is to understand the groundwater evolutionary pattern influenced by  
21 transgression/regression events in geologic time. The findings will be significant to  
22 aquifer remediation activities in the region as well as other similar sedimentary

1 environments around the world.

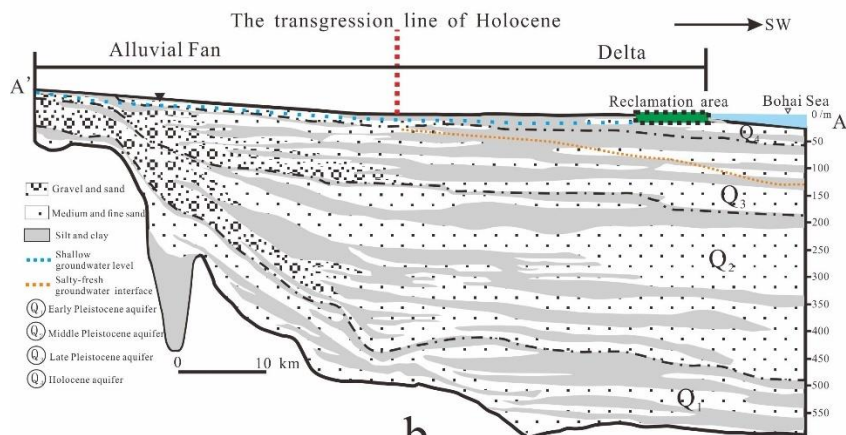
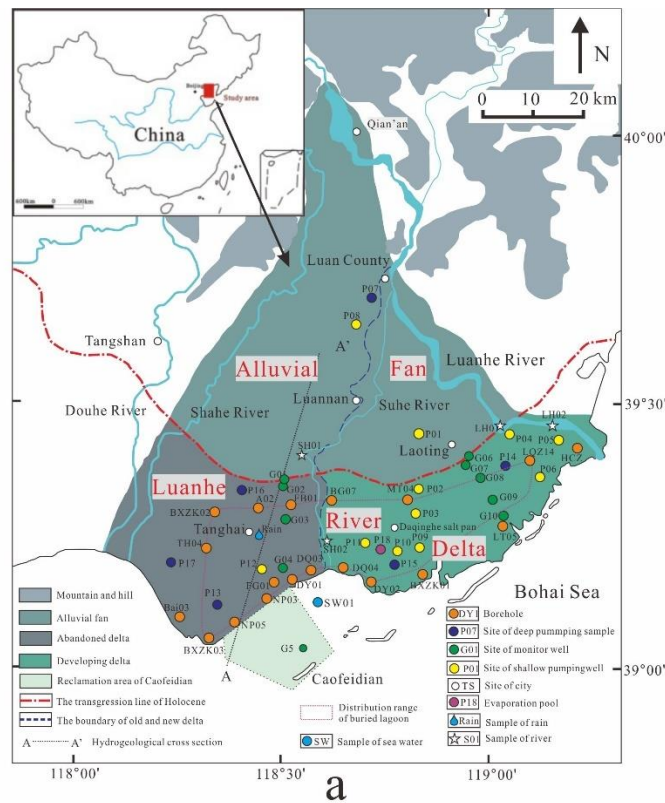
## 2 **2 Background of the study area**

3 The study area is located in northeastern Hebei Province, China, on the west coast of  
4 Bohai (Fig. 1a). The study area consists of alluvial fan and coastal delta, bounded by  
5 Holocene maximum transgression line (Xue et al., 2016). The delta area can be further  
6 divided into two parts: old delta between the Douhe River and the Suhe River, the new  
7 delta between the Suhe River and the modern Luanhe River (He et al., 2020). The  
8 geomorphology of the study area is inclined to the south and southwest with a slope of  
9 about 0.04-2‰. The temperate monsoon climate affects the average annual temperature  
10 of 12.5°C and annual rainfall of 601 mm (1956-2010), with 80% of the annual rainfall  
11 occurring between July and September.

### 12 2.1 Hydrogeology

13 The thickness of Quaternary sediments in the study area is about 400-500 m.  
14 According to the lithology and hydrogeological characteristics, the Quaternary aquifers  
15 are made up of four distinct aquifers (Fig. 1b): the First Holocene aquifer ( $Q_4$ ) is a  
16 phreatic or semi-confined aquifer with a bottom depth of 15-30 m and is primarily  
17 composed of fine sand and slit, involving fresh, brackish, saline and brine groundwater  
18 (Dang et al., 2020). The second Late Pleistocene aquifer ( $Q_3$ ), the third Middle  
19 Pleistocene aquifer ( $Q_2$ ), and the fourth Early Pleistocene aquifer ( $Q_1$ ), with bottom  
20 depths of 120-170 m, 250-350 m, and 350-550 m, respectively. They have confined  
21 aquifers primarily made up of medium sand and gravel (Niu et al., 2019). The first  
22 aquifer is mainly recharged by meteoric precipitation and lateral infiltration of surface

1 water (Li et al., 2013). In the alluvial fan areas, the groundwater from the first aquifer  
 2 is widely extracted for irrigation. The largest salt farm in north China, the Daqinghe  
 3 Salt Farm, uses shallow brine groundwater for salt production in the delta area, where  
 4 agricultural activities are small. Except for the area of alluvial fan, the circulation  
 5 between phreatic and confined aquifers is weak. The deep groundwater in second, third,  
 6 and fourth aquifers are mainly recharged by a surrounding mountain range and mainly  
 7 discharged by human pumping (Ma et al., 2014).



1 Fig. 1. (a) Location map of study area. Also shown are the sampling site and published cores in the  
2 Luanhe River Delta. Cores LT05, HCZ, BXZK01, BXZK02 and BXZK03 were cited from He et  
3 al. (2020); Cores NP05, NP03, DY01, DQ03, DQ04, DY02, MT04, BG07, FB01, A02 and TH04  
4 were cited from Xu et al. (2020); Core LQZ04 was cited from Cheng et al. (2020); Core FG01 was  
5 cited from Xu et al. (2011); Core Bai03 was cited from Li and Wang. (1983); Core HCZ was cited  
6 from Peng et al. (1981). (b) Hydrogeological cross-section (A-A' in Fig. 1a) of study area,  
7 modified by Ma et al., 2014.

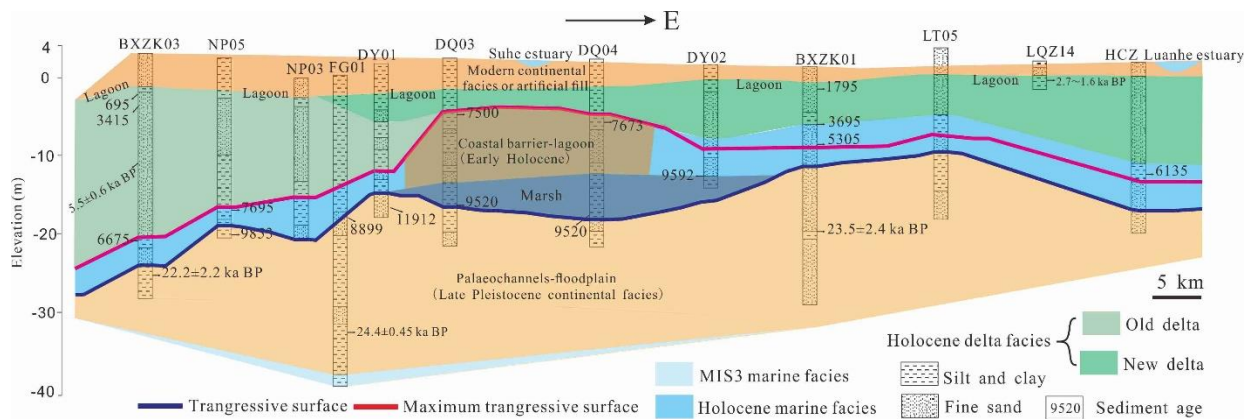
## 8 2.2 Sedimentary evolution since the Late Pleistocene

9 Previous studies have shown that in the study region, the interface of salt-fresh  
10 groundwater gradually deepens from land (depth of ~ -5 m) to sea (depth of ~ -100 m),  
11 as shown in Fig. 1b, with salt groundwater primarily occurring in the first aquifer of the  
12 delta area (Li et al., 2013; Ma et al., 2014). According to stratigraphic transect along  
13 the present coastline (Fig. 2), the series stratigraphic architecture of the first aquifer  
14 consists of Late Pleistocene continental facies - Holocene marine facies – Holocene  
15 delta facies - modern continental facies or artificial fill, indicating that the sediments of  
16 the first aquifer had been deposited from lowstand continental accumulation to marine  
17 transgression and high stand progradation since the Late Pleistocene.

18 The seawater had not reached the modern coastline from the Last Glacial Maximum  
19 to the early Holocene (about 30-9 ka B.P.). The Luanhe alluvial fan was an activity in  
20 this period (He et al., 2020). Since about 9000 a B.P., the Holocene marine transgression  
21 had approached the present coastline (Xu et al., 2020), and Holocene marine sediments  
22 developed under the sea-level rise condition from 9-7 ka B.P. The Holocene marine



1 transgression had reached its maximum inland area 20 km from the modern coastline  
 2 until about 7 ka B.P. (Gao et al., 1981; Peng et al., 1981; Xue, 2014, 2016) (Fig. 1  
 3 transgression line of Holocene), the accumulation of highstand prograding delta on top  
 4 of Holocene marine strata, together with the artificial fill formed the modern coastal  
 5 plain. In addition, lagoons are important components of the Luanhe River Delta (Feng  
 6 and zhang, 1998). According to the records of lagoon facies in the published cores in  
 7 this region, the approximate distribution range of buried lagoon is shown as a purple  
 8 dashed line in Fig. 1a.



9  
 10 Fig.2 Stratigraphic transect along the present coastline of Luanhe River Delta, modified from He  
 11 et al.,2020.

### 12 3 Methods

13 In total, 45 water samples were collected from the Luanhe River Delta, including  
 14 38 groundwater samples, 5 surface water samples, 1 local rain water and 1 Bohai  
 15 seawater samples, during 4 sampling campaigns from October 2016 to June 2020.  
 16 Groundwater samples were divided into shallow groundwater samples and deep  
 17 groundwater samples, which were pumped from unconfined aquifer and confined  
 18 aquifer respectively. Surface water includes 2 Suhe River water samples and 2 Luanhe

1 River water samples. Due to artificial fill that has modified the coastal landscape, it was  
2 difficult to locate the modern lagoon environment. However, during the investigation,  
3 it was found that the Daqinghe salt farm in this area extracts seawater into the  
4 evaporation pond. The mixture of seawater and meteoric water is subject to evaporation  
5 to form concentrated saline water (CSW) in the pond, which is similar to the formation  
6 of CSW in a coastal lagoon (Stumpp et al., 2014). Thus, 1CSW (P18 sample) in the  
7 evaporation pond was collected.

8 Water types were classified according to Zhou (2013): freshwater (TDS < 1 g/L),  
9 brackish water (TDS = 1 to 3 g/L), saline water (TDS = 3 to 50 g/L), and brine (TDS >  
10 50 g/L). Groundwater sampling depths and pH values were measured on site using  
11 CDT-divers. The concentrations of  $K^+$ ,  $Na^+$ ,  $Ca^{2+}$ ,  $Mg^{2+}$ , and  $Br^-$  ion were measured  
12 using inductively coupled plasma analysis (ICAP-7400), while  $SO_4^{2-}$  and  $Cl^-$  ions were  
13 determined using ion chromatography (ICS-600). The  $HCO_3^-$  concentrations of samples  
14 were measured using titration. The hydrochemical data are listed in Table S1(see  
15 Supplement). The stable isotope concentrations ( $\delta D$ ,  $\delta^{18}O$ ) of the water samples  
16 (including G02-10, G06-10, G03-05, G04-40, G05-10, G05-46, G07-27, P07-20, P08-  
17 30, P09-30, P10-30, P11-20, P12-40 P14-15, P07-100, P13-200, P14-300, P15-150,  
18 P16-100, P17-200, P18, LH01, LH02, SH01, SH02, SW01, R1) were tested at the  
19 Experimental & Testing Center of Marine Geology, Ministry of Natural Resource,  
20 China, using High Temperature Pyrolysis-Isotope Ratio Mass Spectrometry. The values  
21 of  $\delta^{18}O$  and  $\delta D$  were calculated with respect to the Vienna Standard Mean Ocean Water  
22 (VSMOW), and the uncertainty for  $\delta D$  and  $\delta^{18}O$  are  $\pm 1.0\%$  and  $\pm 0.2\%$ , respectively.

1 The radioisotope (AMS  $^{14}\text{C}$ ) of groundwater samples (P14-300, P15-150, and P16-100)  
2 were measured at the Pilot National Laboratory for Marine Science and Technology.  
3 Stable isotopes ( $\delta \text{D}$ ,  $\delta \text{ }^{18}\text{O}$ ,  $^{13}\text{C}$ ) and radioisotope of groundwater samples (G10-10,  
4 G03-20, G04-15, G05-30, G06-15, G07-15, G08-15, G08-40, G09-15, G09-40, G10-  
5 10, G10-30) were analyzed at the Beta Analytic TESTING LABORATORY, where the  
6  $\delta \text{ }^{18}\text{O}$  and  $\delta \text{D}$  values were also calculated with respect to VSMOW, and the uncertainty  
7 for  $\delta \text{D}$  and  $\delta \text{ }^{18}\text{O}$  are listed in Table S1. The ~~age of groundwater~~  $^{14}\text{C}$  age of groundwater  
8 was calculated using the following equation:  $t = -8267 \cdot \ln(a_t \text{ }^{14}\text{C} / q \cdot a_0 \text{ }^{14}\text{C})$  (Clark  
9 and Fritz, 1997), where  $t$  is radiocarbon ages in years Before Present (a B.P. );  $a_t \text{ }^{14}\text{C}$  is  
10 the measured  $^{14}\text{C}$  activity in % of modern carbon (pMC);  $a_0 \text{ }^{14}\text{C}$  is the modern  $^{14}\text{C}$   
11 activity of soil derived;  $q$  is a corrective factor, the corrective factor accounts for the  
12 dissolution of calcite, which is assumed to be free of  $^{14}\text{C}$  and, therefore, dilutes the  
13 initial  $^{14}\text{C}$  activity of aqueous DIC in recharged water. The results of  $^{13}\text{C}$ ,  $^{14}\text{C}$  and the  
14 uncorrected residence times are listed in Table S2.

## 15 **4 Results**

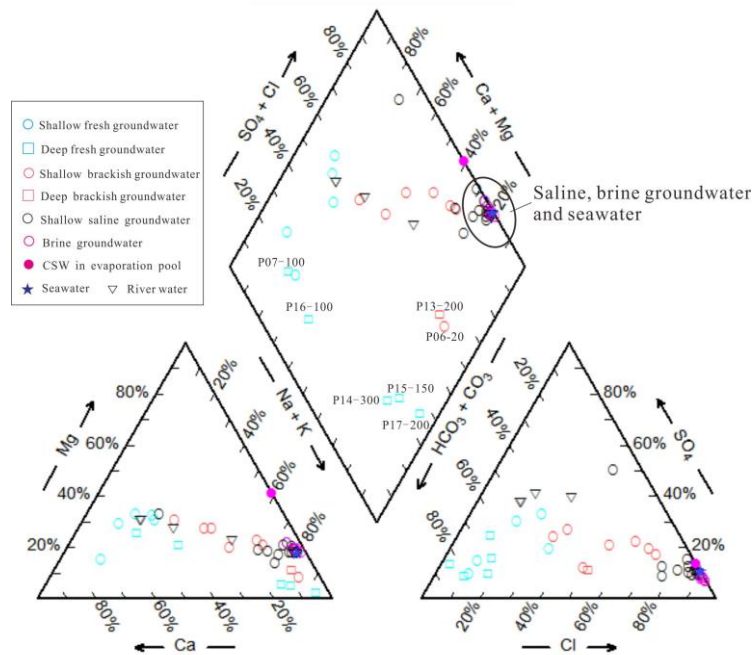
### 16 4.1 Hydrochemistry

17 Except for P13-200 (TDS=1.617 g/L, which is brackish water), all the deep  
18 groundwater samples in the study region are freshwater. Deep groundwater  
19 hydrochemical forms shift from  $\text{Ca-HCO}_3$  to  $\text{Na-HCO}_3$  as it moves from land to sea  
20 (Fig. 3). For shallow aquifer, the horizontal interface of salt-fresh groundwater  
21 corresponds better with the maximum Holocene transgression line (see Fig. 1a). The  
22  $\text{Ca-HCO}_3$  type of shallow fresh groundwater is primarily distributed in the alluvial fan

1 region. The brackish and low TDS saline groundwater, which vary from Ca-HCO<sub>3</sub>, Na-  
2 HCO<sub>3</sub>, and Na-Cl types, are mainly contained in the upper aquifer (depth of 0-15 m) of  
3 delta area, while the lower part (depth of 20–40 m) is Na-Cl type of saline and brine  
4 groundwater with high TDS. Moreover, for horizontal distribution of salinity, the  
5 groundwater TDS tends to decrease from west to east, such as the TDS of saline and  
6 brine groundwater TDS generally range from 16.57–125.97 g L<sup>-1</sup> in old delta (western  
7 delta), while 3.26–52.48 g L<sup>-1</sup> in the new delta (eastern delta).

8

1



2

3

Fig. 3 Piper diagram of the various water samples.

4

#### 4.2 $^2\text{H}$ , $^{18}\text{O}$ stable isotopes

5

6

7

8

9

10

11

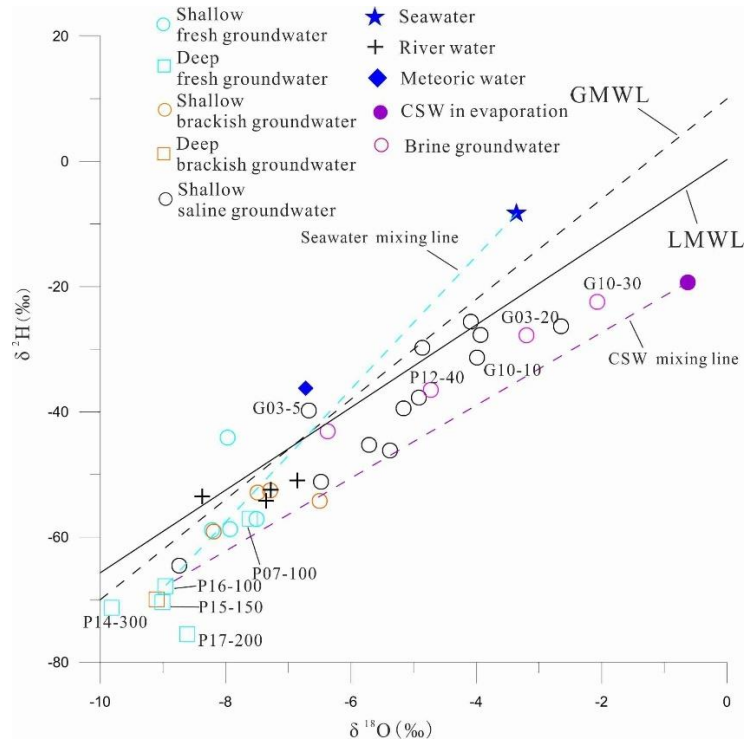
12

13

14

Fig. 4 shows the relationship between deuterium and oxygen-18. The global meteoric water line (GMWL,  $\delta^2\text{H}=8\cdot\delta^{18}\text{O}+10$ ) is cited from Craig (1961), while the local meteoric water line (LMWL,  $\delta^2\text{H}=6.6\cdot\delta^{18}\text{O}+0.3$ ) is based on  $\delta^2\text{H}$  and  $\delta^{18}\text{O}$  isotope data (1985-2003, mean monthly rainfall values) from the Tianjin station, about 100 km southwest of the study area (IAEA/WMO, 2006). The deep groundwater samples exhibit depleted values of stable isotopes, with values of  $\delta^2\text{H}$  ranging from -75.52‰ to -57.06‰ and  $\delta^{18}\text{O}$  from -9.82‰ to -7.61‰. Shallow groundwater samples have higher hydrogen and oxygen isotope levels, ranging from -64.6 to -22.46‰ for  $\delta^2\text{H}$  and -8.74 to -2.07‰ for  $\delta^{18}\text{O}$ . While the relatively small overall value of fresh and brackish groundwater samples are similar to those of the river samples saline and brine

1 groundwater, were generally plotted below the LMWL or GMWL, which mean that the  
 2 water was subjected to evaporation prior to recharge into groundwater (Gibson et al.,  
 3 1993), or that multiple end-members mixing processes were involved (Han et al., 2011).



4  
 5 Fig. 4 Stable isotope compositions of different water samples. Seawater mixing line: mixing  
 6 between deep fresh groundwater and seawater; CSW mixing line: mixing between deep fresh  
 7 groundwater and CSW.

#### 8 4.3 Groundwater residence times

9 The measured  $^{14}\text{C}$  activities of groundwater samples range from 0.774 to 105.9 pMC  
 10 (Table S2). The properties of  $^{14}\text{C}$  and sampling depth is shown in Fig. 5, which  
 11 elucidates the negative correlations, showing that variations of  $^{14}\text{C}$  activities could be  
 12 attributed to radioactive decay aquifer. There are multiple processes that can impact the  
 13  $^{14}\text{C}$  properties including groundwater mixing and dispersion, long-term variation of  
 14 atmospheric  $^{14}\text{C}$  and free  $^{14}\text{C}$  dilution (e.g. carbonate dissolution) (Cartwright et al.,

1 2020). Due to the relative impact of these processes (which are not well established  
2 in the study area), the uncertainty regarding the correction of radiocarbon ages to real  
3 groundwater ages is very high. Consequently, we estimate groundwater age as a range  
4 of the residence time. Uncorrected ages are considered the maximum age, while  
5 corrected ages are the minimum age that are determined based on two hypothetical  
6 models on carbonate dissolution that mainly affect the  $^{14}\text{C}$  contents of water samples  
7 (Lee et al., 2016).

8 Fig.5 shows activities of the  $^{14}\text{C}$  in the shallow groundwater are within 30.6 to 105.9  
9 pMC. These values indicate relatively modern recharge before atmospheric nuclear  
10 testing period of the 1950s and 1960s. The radiocarbon activities in the deep fresh  
11 groundwater are less than 12 pMC, which is consistent with the palaeo-water recharge.  
12 This indicates that there are weak connection between shallow and deep aquifers.  
13 Therefore, we assume that the shallow aquifer is an open system, while the deep aquifer  
14 is a closed system. The  $\delta^{13}\text{C}$  mixing and chemical mass balance (CMB) models are used  
15 to estimate to corrective factor  $q$ , respectively (Clark and Fritz, 1997).

16 For  $\delta^{13}\text{C}$  mixing model,  $q = (\delta^{13}\text{C}_{\text{DIC}} - \delta^{13}\text{C}_{\text{CARB}}) / (\delta^{13}\text{C}_{\text{RECH}} - \delta^{13}\text{C}_{\text{CARB}})$   
17 (Pearson and Hanshaw, 1970), where  $\delta^{13}\text{C}_{\text{DIC}}$  is the measured  $\delta^{13}\text{C}$  of DIC in  
18 groundwater;  $\delta^{13}\text{C}_{\text{CARB}}$  is the  $\delta^{13}\text{C}$  of DIC from dissolved soil mineral, using  $\delta^{13}\text{C}_{\text{CARB}}$   
19 = 1.5 ‰ (Chen et al., 2003);  $\delta^{13}\text{C}_{\text{RECH}}$  is the  $\delta^{13}\text{C}$  in water when it reaches the saturation  
20 zone. In this study, we use a  $\delta^{13}\text{C}_{\text{RECH}}$  of -15 ‰, which has been suggested as  
21 appropriate for soils in northern China dominated by  $\text{C}_4$  plants (Currell et al., 2010).  
22 The model yielded some relatively low  $q$  values (0.59 of G06-15 and 0.65 of G08-15),

1 possibly since several unaccounted factors would contribute to variable  $\delta^{13}\text{C}_{\text{RECH}}$  values,  
2 e.g. local methanogenesis and pH or temperatures in the soil zones.

3 For CMB,  $q = \text{mDIC}_{\text{rech}} / \text{mDIC}_{\text{final}}$ , where  $\text{mDIC}_{\text{rech}}$  is the DIC molar concentration  
4 in the recharging water and  $\text{mDIC}_{\text{final}}$  is the DIC molar concentration in the final  
5 groundwater.  $\text{mDIC}_{\text{final}}$  was calculated using:  
6  $\text{mDIC}_{\text{final}} = \text{mDIC}_{\text{rech}} + [\text{mCa} + \text{Mg} - \text{SO}_4 + 0.5(\text{Na} + \text{K} - \text{Cl})]$  (Fontes and Garnier,  
7 1979).  $\text{mDIC}_{\text{rech}}$  was estimated based on groundwater pH and temperature in the  
8 assumed recharge area, e.g.,  $\text{mDIC}_{\text{rech}} = 10 \text{ mmol/L}$  for  $\text{pH} = 6$  and  $T = 15^\circ\text{C}$  (Han et  
9 al., 2011).

10 The corrected radiocarbon ages are shown in Table S2. ~~and~~ The residence time of  
11 deep groundwater ranged from 15959-39050 a B.P., which is significantly longer than  
12 that of groundwater in the shallow aquifer (~~about~~ 9510 a B.P. to modern). Moreover,  
13 the ages of most brackish and fresh groundwater are modern, while brine has a longer  
14 residence period (~~about 1.2-4.3 cal ka~~ 5590-1245 a B.P.) and a broader variety of saline  
15 groundwater samples.



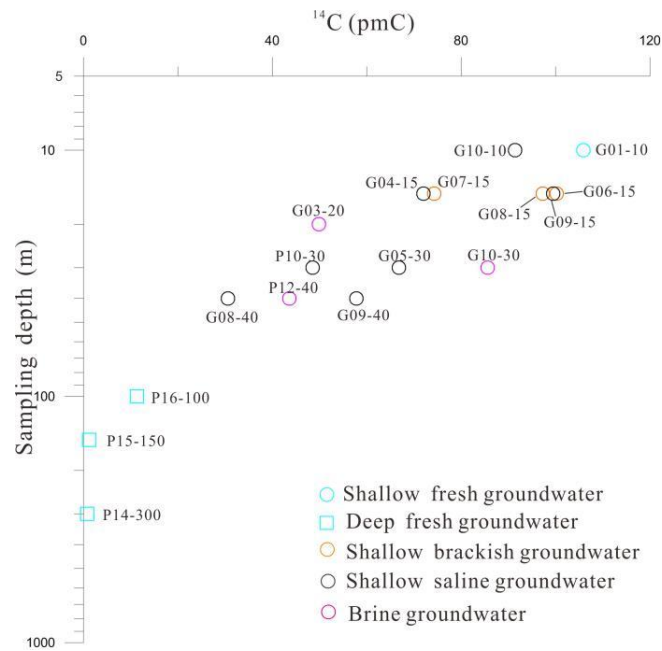


Fig. 5  $^{14}\text{C}$  activity with sampling depth in groundwater.

## 5 Discussion

### 5.1 Isotopic analysis for origin and recharge of groundwater

Deuterium and oxygen-18 are good tracers for groundwater origin and climatic conditions during recharge periods (Clark and Fritz, 1997). When combined with groundwater residence time, they could further identify modern and palaeo recharge (Han et al., 2014).

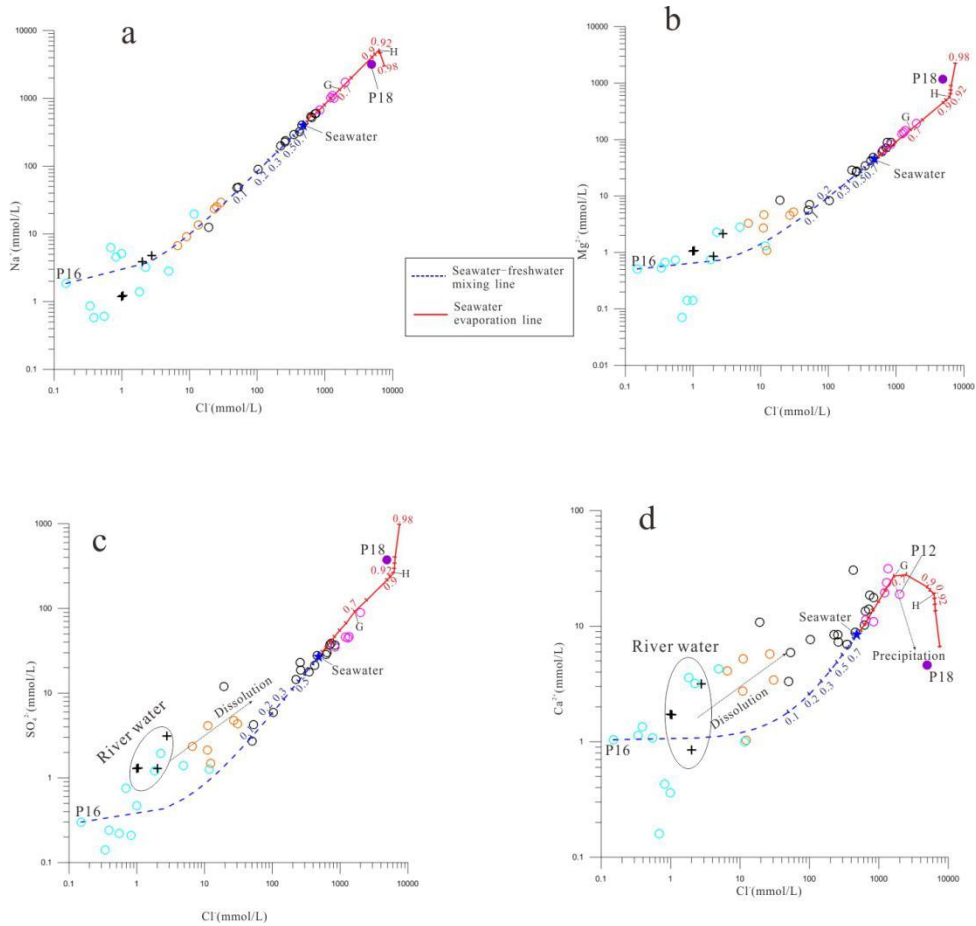
The depletion of  $^{18}\text{O}$  and  $^2\text{H}$  values in the deep fresh groundwater (Fig. 4) can be attributed to a cold climate (Kreuzer et al., 2009) and residence time of P15-150 and P14-300 samples (range from 33951 to 39050 a B.P) which may suggest that there was a recharge during the last glacial maximum. The stable isotopes of P16-100 are more enriched, reflecting recharge history of warm climate during the last deglaciation (Hendry and Wassenaar, 2000). The stable isotope values of river samples are similar to those of the shallow brackish and fresh groundwater compositions of the approximate

1 modern age, indicating lateral recharge of surface water locally. Meanwhile, in Fig. 4,  
2 G03-5 is close to the rainfall sample, indicating that modern precipitation is a new  
3 recharge source. The trend toward  $\delta^{2}\text{H}$  and  $\delta^{18}\text{O}$  enrichment in brine and saline  
4 groundwater could be attribute to infiltration of seawater during Holocene transgression  
5 period, which has been confirmed by other study in Bohai Sea coast (Li et al., 2017, Du  
6 et al., 2016). Additionally, due to mixing of meteoric water, and the subsequent non-  
7 equilibrium fractionation of hydrogen isotope during evaporation (Clark and Fritz,  
8 1997), the CSW sample is characterized by  $^{18}\text{O}$  enrichment compared to seawater but  
9  $^{2}\text{H}$  depletion.

## 10 5.2 Hydrochemical analysis for sources of salinity

11 For distinguishing the sources of groundwater salinity, the PHREEQC code (Parkurst  
12 and Appelo, 2013) was used to measure and plot the theoretical seawater-freshwater  
13 mixing line (“mixing line”) and seawater evaporation line (“evaporation line”) using  
14 hydrogeochemical modeling. Using both simulation effects as references to  
15 groundwater hydrochemical characteristics (Figs. 6 and 7. For the Na-Cl (Fig. 6a), Mg-  
16 Cl (Fig. 6b), and Br-Cl (Fig. 7a) diagrams, whose measured brackish, saline and brine  
17 groundwater samples fit quite well to modeling mixing lines and evaporation lines  
18 follow linear trends from the least to the most saline. This would strongly demonstrate  
19 that, the salt in these water samples is mainly of marine origin. The major ions  
20 concentration in some samples (such as brine) are higher than those in the seawater,  
21 suggesting the enriched ions are associated with evaporation processes, rather than  
22 seawater intrusion (Colombani et al, 2017).

1        Moreover, the samples deviate from the modeling lines (Fig. 6c and 6d), indicating  
2        that there may be other hydrogeochemical processes responsible for the modified ionic  
3        compositions (Giambastiani et al., 2013): (1)  $\text{Ca}^{2+}$  depletion of P18 and P12 samples  
4        are shown in Fig. 6d. This phenomenon is likely explained by gypsum ( $\text{CaSO}_4$ )  
5        precipitation. The evaporation line reveals that the  $\text{Ca}^{2+}$  composition of evaporating  
6        seawater follows a hooked trajectory (Fig. 6d). During evaporation to the point of  
7        gypsum saturation, residual CSW becomes progressively decreased  $\text{Ca}^{2+}$  concentration.  
8        (2)  $\text{Ca}^{2+}$  and  $\text{SO}_4^{2-}$  excess in most fresh and brackish samples (Fig. 6c and d) could be  
9        attributed to mineral dissolution along with stream water recharging, highlighting some  
10       degree of dilution with continental runoff since Holocene regression. (3)  
11       Decomposition of organic matters which are abundant in marine or lagoon facies  
12       sediments can result in release of bromide ions, and thus making the Br/Cl ratios of  
13       saline groundwater samples higher than the mixing line (Fig. 7b).



1

2 Fig. 6 Hydrochemical relationship between Cl and major ions of measured samples and simulated

3 results (seawater-freshwater mixing line: theoretical mixing between seawater and deep fresh

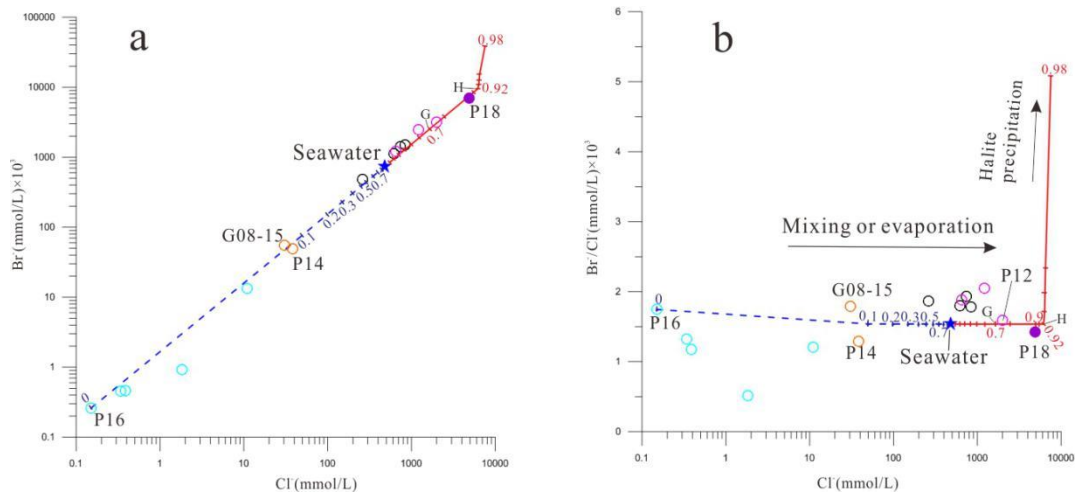
4 groundwater, and the blue numbers are mixing ratios of seawater; seawater evaporation line:

5 theoretical evaporation of Bohai seawater, and the red numbers are different evaporation rates) in

6 groundwater. G and H stand for point of precipitation of gypsum, halite respectively. The symbols

7

of samples are same as Fig. 6.



1

2 Fig. 7 Relationship between chloride and bromide content in water samples. Symbols are same as

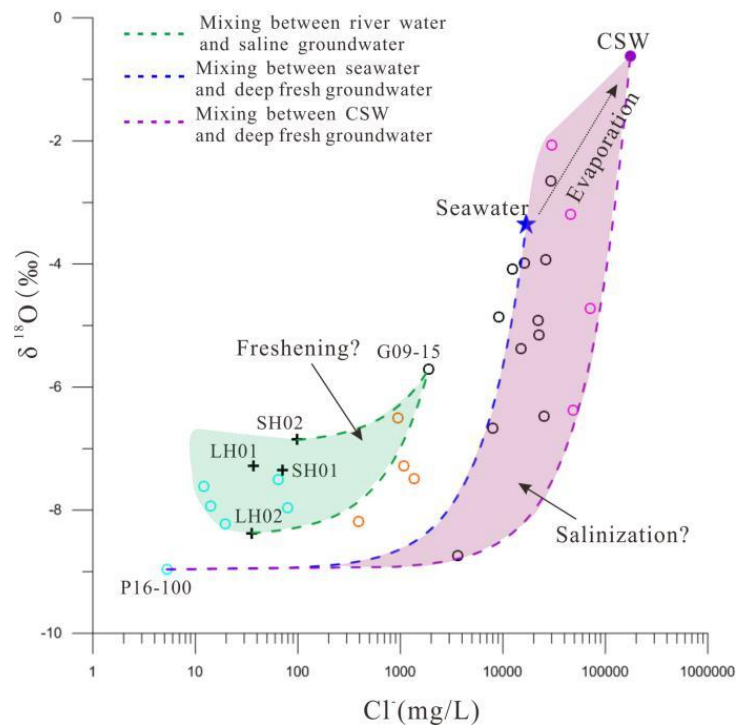
3

Fig. 6.

4 5.3 Mixing processes

5 Fig. 8 depicts the relationship between  $\delta^{18}\text{O}$  and  $\text{Cl}^-$  in different water samples. In  
 6 brine samples, there is a higher  $\text{Cl}^-$  concentration and lower  $\delta^{18}\text{O}$  values than in seawater,  
 7 meaning that simple two end-members mixing cannot adequately explain groundwater  
 8 salinization. Stable isotopes of high TDS saline and brine samples fall between the  
 9 seawater and CWS mixing lines, further suggesting potential three end-member mixing  
 10 processes (Douglas et al., 2000). Therefore, we considered SW01 (seawater but with  
 11 most enriched  $\delta^{18}\text{O}$ ) and P18 (most saline but with relatively depleted  $\delta^{18}\text{O}$ ) as two  
 12 saline end-members. The P16-100, which is most likely recharged during the Last  
 13 Deglaciation, was chosen to represent fresh end-members that could have been  
 14 impacted by overlying seawater or CSW during Holocene transgression.-In Fig. 8, an  
 15 inferred salinization zone was established that included almost all saline and brine  
 16 groundwater samples, demonstrating the salinization processes in which fresh  
 17 groundwater mixed with either seawater, CSW, or a mixture of both.

1 The fresh and brackish groundwater samples, on the other hand, have low  $\text{Cl}^-$   
 2 concentrations and depleted  $^{18}\text{O}$ , deviating from the assumed salinization zone but  
 3 approaching the river samples in Fig. 8, implying a river water-groundwater mixing  
 4 trend. The LH02 (depleted  $\delta^{18}\text{O}$ ) and SH02 (relatively enriched  $\delta^{18}\text{O}$ ) were selected to  
 5 represent river water end-members range for different continental runoff in study area,  
 6 while the G09-15 (saline but with river-like stable isotope) was considered as a  
 7 groundwater end-member. There is a presumed freshening zone could form between  
 8 two river water-groundwater mixing lines, indicating occurrence of freshening  
 9 processes which would be in agreement with continental runoff dilution discussed in  
 10 section 5.2.



11  
 12 Fig. 9 8 Relationship between  $\text{Cl}$  and  $\delta^{18}\text{O}$  of different water samples as means to various mixing  
 13 processes in the Luanhe River Delta. The symbols are same as Fig. 6. The green area is assumed  
 14 freshening zone, and the purple area is assumed salinization zone.

## 1 **6 Interpretation of palaeo-environmental development**

2 Based on analysis of a range of evidence related to Quaternary geographic evolution,  
3 it is possible to understand the change of hydrogeological conditions in the past (Van  
4 Engelen et al., 2018). The Pleistocene transgression events-related to Marine isotope  
5 stage (MIS) 3 and 5-have been observed to once reach the study area by other authors  
6 (Wang et al., 1981; Peng et al., 1981; Li et al., 1982; Xu et al., 2018,), which would be  
7 resulted in groundwater salinization. Since the last deglaciation (about 15 ka B.P.), the  
8 palaeo-coast line has approximately 100 m depth below present sea level along the shelf  
9 edge (Liu et al., 2020; Li et al., 2014). Stronger river down-cutting and flushing in the  
10 study region would have been helped a large fresh recharge of groundwater. For  
11 example, P16-100 (fresh water) was sampled from a relatively deep position (100 m  
12 below surface) has an estimated groundwater age between 15959 to 17490 a B.P., which  
13 is likely to provide evidence that the salinization groundwater related to MIS 5 and/or  
14 3 marine transgression could have been flushed out until the Latest Pleistocene.  
15 Accordingly, we believe that the observed saline groundwater in the Luanhe River Delta  
16 is probably related to the subsequent Holocene marine transgression. This research  
17 develops the evolutionary pattern of saline groundwater, as shown in Table 1 and Fig.  
18 three phases are synthesized and reconstructed, as follows.

19

1 Table 1 Saline groundwater evolution processes in study area

Evolution stage	Groundwater evolution processes		Influencing factors			Major hydrogeochemical processes	Sediments	
	Evolutionary pattern	Factors	Palaeoclimate	Geological setting	Others			
Phase 3 The development of new delta (3.5ka B. P. to present)	Freshening	Wash-out of surface water	temperate, slightly semi-humid	Development of surface stream	irrigation return	Mixing and leaching		Holocene alluvial deposit or artificial fill Bottom sediments age about 1795–302 a B. P. (Xu et al., 2020; He et al., 2020)
	Deceleration of brine formation	Limitations of seawater evaporation		Diversion of channels and lagoon filled by diluvial deposit	artificial reclamation and offshore levees			
Phase 2 The development of old delta (7 to 3.5ka B. P.)	Brine formation	Seawater evaporation and CSW infiltrating	temperate, slightly arid	Deceleration of sea-level rising, development of delta, and coastal lagoons have been active	Tides or storm	Mixing, leaching, evaporation, and mineral precipitation		Holocene delta facies Bottom sediments age about 6675–3695 a B. P. (He et al., 2020)
Phase 1 Holocene transgression (12 to 7ka B. P.)	Groundwater salinization	Palaeo-seawater intrusion	temperate-warm humid	Deglaciation of ice sheet, rapid rising of sea level, Holocene transgression		Mixing		Holocene marine facies Bottom sediments age about 8620–5595 a B. P. (Li et al., 1982)
								Late Pleistocene continental facies (Xu et al., 2020; He et al., 2020)

2  
3 *Phase 1: Transgressive system tract-Holocene transgression stage (9-7 ka B.P.)*

4 Global sea level was affected by deglaciation of the ice sheet (Fairbanks, 1989),  
5 causing sea level to rise rapidly during the deglaciation period (15.4-7 ka B.P.) (Li et  
6 al., 2014). It could be summarized that the Holocene transgression stage, which  
7 occurred between 9 and 7 ka B.P, resulted in the study area being inundated by seawater  
8 (Xu et al., 2015; Xue 2009, 2014) (Fig. 9a). On the one hand, there would have been a  
9 tendency for the denser seawater to infiltrate through the aeration zone (Santucci et al.,  
10 2016); on the other hand, sea-level rise would cause the seawater-freshwater interface  
11 to move landward (Ferguson and Gleeson, 2012), both of which contributed to palaeo-  
12 seawater intrusion. The G08-40 contains TDS of 27.173 g/L, which is more similar to  
13 that of SW01. Simultaneously, the residence time (9810-6884 a B.P.) indicate trapped  
14 palaeo-seawater at low-permeability aquitard sediments still exists and may be another  
15 critical salinity source for neighboring aquifers in the coastal zone (Post and Kooi, 2003;  
16 Lee et al., 2016).

17 The presence of palaeo-seawater intrusion during Quaternary has been recorded in  
18 other coastal regions worldwide (Groen et al., 2000; Bouchaou et al., 2009, Tran et al.,



1 2012; Delsman et al., 2014; Han et al., 2020). For the works described above, the  
2 salinity of groundwater after salinization could not exceed that of seawater due to  
3 palaeo-seawater intrusion.

4 Other salinization processes that occurred during palaeo-environmental growth are  
5 likely to be correlated with such brine groundwater.

6 *Phase 2: Highstand system tract-Old Luanhe River Delta development (7-3.5 ka B.P.)*

7 The good fit between the measured hydrochemistry and simulated evaporation lines  
8 (Fig. 6 and 7) is an indicator that the brine samples were associated with the seawater  
9 which was exposed to evaporation during geological history. Previous research has  
10 revealed that lagoon was active during the progradation of the old Luanhe River Delta  
11 between 7 and 3.5 ka B.P. (He et al., 2020; Xu et al., 2020). Meanwhile, the relatively  
12 arid climate had been developed since 5500 a B.P., which may lead to increased  
13 evaporation (Jin, 1984). The ancient lagoon would be an ideal location for evaporating  
14 seawater that had been trapped due to storms or tides (Fig. 9b). As a result, concentrated  
15 saline water (CSW) with salinity higher than seawater would have created, and the  
16 CSW would go through two processes: (1) infiltrating and descending to the lower part  
17 of the aquifer due to its higher density, and combining with the salinized groundwater  
18 from phase 1, resulting in a three end-members mixing scenario in the relationship  
19 diagram (Fig. 8). (2) After reaching saturation during the later stages of evaporation,  
20 mineral precipitation, such as gypsum, calcite, and halite, would occur, and this would  
21 be subjected to redissolution by meteoric waters or seawater, resulting in high salinity  
22 water that would then be subjected to the above process; The Br/Cl ratios in certain

1 fresh or brine groundwater samples deviate from the evaporation line (Fig. 87b), which  
2 may be related to halite precipitation and redissolution. These two processes caused  
3 groundwater salinity to rise even further, resulting in the formation of brine  
4 groundwater with 3 times the TDS of seawater, such as G03-20 with a range of resident  
5 time of 4323 to 5590 a B.P.

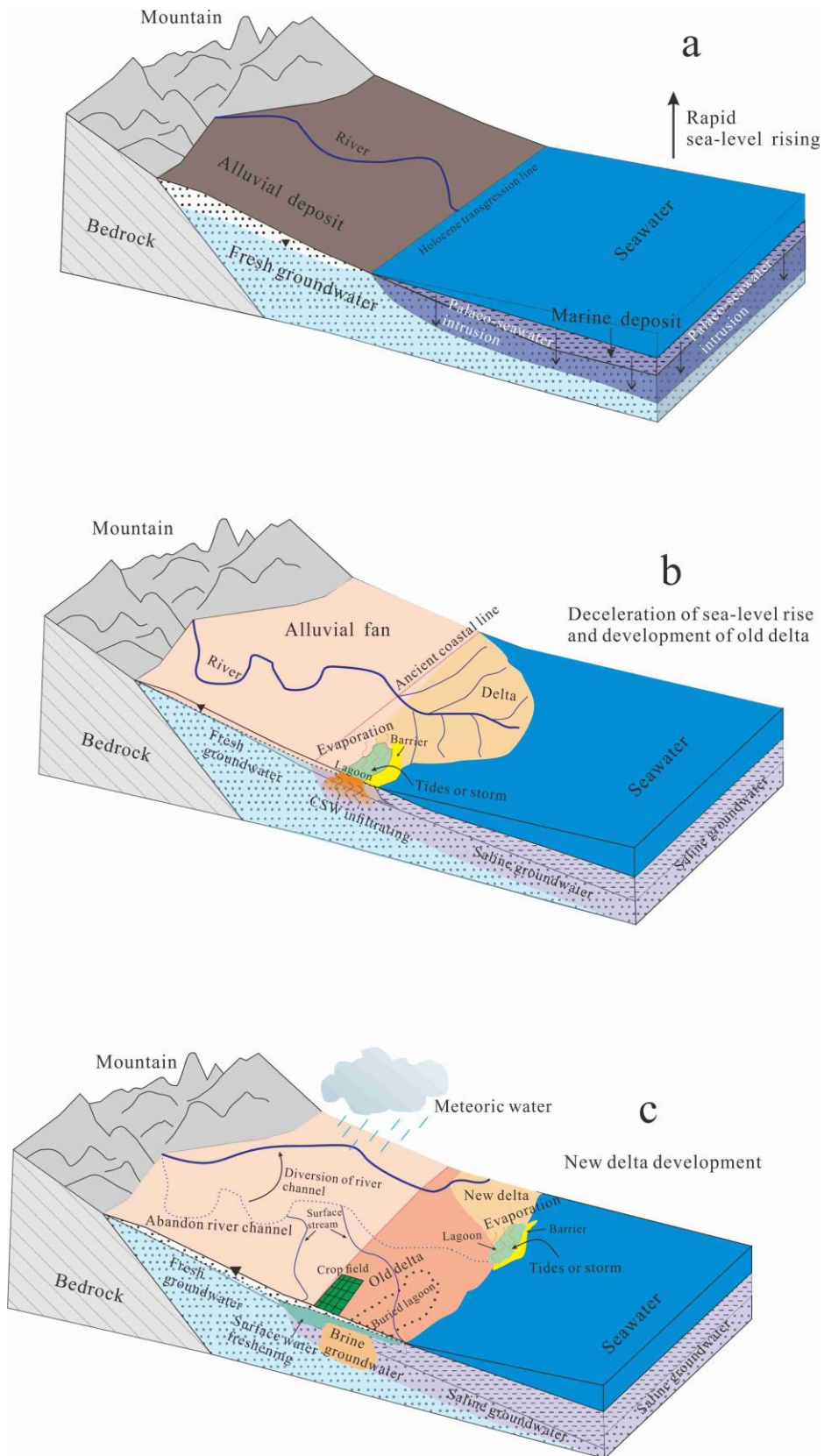
6 *Phase 3: New Luanhe River Delta development (3.5 ka B.P. -present)*

7 Since about 3500 a B.P., a nearly 90-degree diversion of the Luanhe River channel  
8 in the study area resulted in new delta development (Wang et al., 2007; Xue et al., 2016).  
9 There are some signs of a lagoon environment in the new Luanhe River Delta (Cheng  
10 et al., 2020), and, as previously discussed, the brine groundwater sample G10-30 would  
11 be attributed to evaporation in a lagoon setting (Fig. 9c). However, some factors are  
12 likely to limit the CSW formation in the study area: (1) the relatively low evaporation  
13 capacity due to semi-humid climate since about 2.5 ka B.P. (Jin, 1984), (2) the diluvial  
14 deposit or artificial reclamation would have filled the coastal low-land such as lagoons,  
15 and (3) offshore levees prevent the seawater from flooding inland during storms or tides.  
16 These factors may also explain why, unlike the old Luanhe River Delta, the current  
17 Luanhe River Delta does not have high TDS brine groundwater.

18 In addition, the brackish and low TDS saline groundwater with relatively modern age  
19 (e.g. G09-15), and river-like stable isotopes (Fig. 4 and 8), are compelling evidence that  
20 freshening processes have occurred in the delta plain. Since the semi-humid  
21 palaeoclimate, some abandoned channels have developed into small rivers after the  
22 diversion of the ancient Luanhe River (Gao, 1981), such as the Suhe River and Shahe

1 River. Firstly, the lateral recharge from the surface stream plays a role in washing out  
2 the salty groundwater. Secondly, due to the inefficiency of saline groundwater  
3 throughout human history, river irrigation has been commonly used for agricultural  
4 activities in the study region, freshening the upper saline aquifer (Fig. 9c). Some  
5 groundwater samples found above the seawater mixing line in the Ca-Cl and SO<sub>4</sub>-Cl  
6 relationship diagrams (Fig. 6c, d) may be related to mineral dissolution during river  
7 water or irrigation recharge. However, saline groundwater can be washed out over time  
8 in coastal zones with low-permeable marine layers and a low hydraulic gradient (van  
9 Engelen et al., 2019; Han et al., 2020).

10 In summary, the evolution of saline groundwater in the study area is a result of  
11 palaeo-environment development such as sea-level change, palaeogeography, and  
12 palaeoclimate, and is significantly affected by human activities. The coastal brine  
13 groundwater is a special product of geological evolution, which have been found in  
14 Bohai Sea coast such as Bohai Bay (Li et al., 2017) and Laizhou Bay (Han et al., 2014).  
15 The change in sea level over the Late Pleistocene would have favoured marine intrusion  
16 and similar sedimentary environment in Bohai coast, allowing this study infers the  
17 following conditions for its brine formation: (1) stable evaporative environments (e.g.  
18 lagoon), (2) suitable climatic conditions (e.g. arid), (3) seawater entering evaporative  
19 environments (e.g. storm or tide), and (4) long-term scale for salinity accumulation.



1

2 Fig. 9 Diagram of palaeoenvironmental development since Holocene and evolutionary pattern of

3

saline groundwater.

## 1 **7 Conclusions**

2 In this study, we used a range of isotopic-geochemical methods to analyze the  
3 recharge and salinity source of groundwater in the Luanhe River Delta. The isotopic  
4 results ( $^2\text{H}$ ,  $^{18}\text{O}$ ,  $^{14}\text{C}$ ) show that deep confined groundwater was recharged during the  
5 Late Pleistocene cold period, shallow saline and brine groundwater was recharged  
6 during the warm Holocene period, and shallow brackish and fresh groundwater was  
7 mainly recharged by surface water. The hydrogeochemical modeling (PHREEQC)  
8 results show that seawater or evaporated seawater is the primary salty source in  
9 salinized groundwater. The variation in the  $^{18}\text{O}$ -Cl relationship of multiple water  
10 samples further indicates multiple end-member mixing, which is useful to assess the  
11 salinization and/or freshening processes in aquifers. Our study shows that multiple  
12 water types are particularly associated with complex geographic evolution in coastal  
13 areas. The variation in sea-levels (when it rises) causes lowland coastal areas to be  
14 inundated by seawater, which induces palaeo-seawater intrusion. The coastal deltas  
15 developed after significant drop in the sea levels. The concentration of saline water in  
16 the lagoon environment at the delta-front continuously provided salinity to the  
17 groundwater. Thus, under the effects of evaporation, mixing, and dissolution, brine  
18 groundwater was formed. In contrast, the lateral recharge of surface water and irrigation  
19 return would cause slow wash-out of salinized groundwater in the delta plain.

20 Given that most coastal zones around the world experienced transgression/regression  
21 events in the Quaternary period, the findings of this work will promote better  
22 understanding of the origin of salinization in coastal aquifers. In addition, it is important

1 to recognize the potential leak of connate saline groundwater previously preserved in  
2 adjunct aquifers that can occur due to over-extraction of deep groundwater. To  
3 effectively prevent pollution from saline groundwater movement, this study  
4 recommends extensive characterization of groundwater interface dynamics, such as  
5 fresh/saline, fresh/brine, and brine/seawater interfaces and also maintain continuous  
6 monitoring of water quality and levels across the aquifers  
7

1 **Authors contribution**

2 Xianzhang Dang: Conceptualization, Formal analysis, Investigation, 3 Writing-

3 Original Draft, Data curation.

4 Maosheng Gao: Funding acquisition, Methodology, Supervision, Investigation,

5 Writing-Review & Editing.

6 Zhang Wen: Supervision, Writing-Review & Editing.

7 Guohua Hou: Project administration, Investigation.

8 Hamza Jakada: Writing-Review & Editing.

9 Daniel Ayejoto: Writing-Review & Editing.

10 Qiming Sun: Investigation.

11

1 Acknowledgement

2 This study was financially supported by the National Natural Science Foundation  
3 of China (41977173), National Key Research and Development Program of China  
4 (No.2016YFC0402800) and the National Geological Survey Project of China Geology  
5 Survey (No. DD20211401). The authors would like to thank Sen Liu, Chenxin Feng,  
6 Chen Sheng, Xueyong Huang and Haihai Zhuang, for their help and support in  
7 collecting field data and conducting geological survey.



1 **References**

- 2 Akouvi, A., Dray, M., Violette S., et al., 2008. The sedimentary coastal basin of Togo:  
3 example of a multilayered aquifer still influenced by a palaeo-seawater intrusion.  
4 *Hydrogeology Journal*, 16, 419-436, doi: 10.1007/s10040-007-0246-1.
- 5 Aquilina, L., Vergnaud-Ayraud, V., Les Landes, A. A., et al., 2015. Impact of climate  
6 changes during the last 5 million years on groundwater in basement aquifers,  
7 *Scientific Reports*, 5, 14132, doi: 10.1038/srep14132.
- 8 Bouchaou, L., Michelot, J.L., Qurtobi, M., et al., 2009. Origin and residence time of  
9 groundwater in the Tadla basin (Morocco) using multiple isotopic and  
10 geochemical tools. *Journal of Hydrology*, 379, 323-338, doi:  
11 10.1016/j.jhydrol.2009.10.019.
- 12 Cary, L. et al., 2015. Origins and processes of groundwater salinization in the urban  
13 coastal aquifers of Recife (Pernambuco, Brazil): A multi-isotope approach.  
14 *Science of the Total Environment*, 530-531, 411-429, doi:  
15 10.1016/j.scitotenv.2015.05.015.
- 16 Cartwright, I., Currell, M., Cendon, D., Meredith, K., 2020. A review of the use of  
17 radiocarbon to estimate groundwater residence times in semi-arid and arid areas.  
18 *J. Hydrol.*, 580, 124247. <https://doi.org/10.1016/j.jhydrol.2019.124247>.
- 19 Chen, Z.Y., Qi, J.X., Xu, J.M., Xu, J.M., Ye, H., Nan, Y.J., 2003. Paleoclimatic  
20 interpretation of the past 30 ka from isotopic studies of the deep confined aquifer  
21 of the North China Plain. *Applied Geochemistry*, 18, 997-1009, doi:  
22 10.1016/S0883-2927(02)00206-8.

1 Cheng, L.Y., Xu, Q.M., Guo, H., et al., 2020. The Late Holocene Stratum and evolution  
2 in the Luanhe River Delta. *Quaternary Sciences*, 40(3), 751-763, doi:  
3 10.11928/j.issn.10017410.2020.03.13(In Chinese with English abstract).

4 Clark, I.D., and Fritz, P., 1997. *Environmental Isotopes in Hydrogeology*. Lewis  
5 Publishers, New York.

6 Colombani, N., Cuoco, E., Mastrocicco, M., 2017. Origin and pattern of salinization in  
7 the Holocene aquifer of the southern Po Delta (NE Italy). *Journal of Geochemical*  
8 *Exploration*, 175(2017): 130-137, doi: 10.1016/j.gexplo.2017.01.011.

9 Cost Environment Action 621, 2005. *Groundwater management of karstic coastal*  
10 *aquifers*. European Communities, Luxembourg.

11 Costall A. R., Harris B. D., Teo B., Schaa R., Wagner F.M., Pigois J. P., 2020.  
12 *Groundwater Throughflow and Seawater intrusion in High Quality coastal*  
13 *Aquifers*. *Scientific Reports*, 10: 9866, doi: 10.1038/s41598-020-66516-6.

14 Craig, H., 1961. Standard for reporting concentration of deuterium and oxygen-18 in  
15 natural water. *Science*, 133, 1833-1834, doi: 10.1126/science.133.3467.1833.

16 Currell, M.J., Cartwright, I., Bradley, D.C., Han, D.M., 2010. Recharge history and  
17 controls on groundwater quality in the Yuncheng Basin, north China. *Journal of*  
18 *Hydrology*, 385, 216-229., doi: 10.1016/j.jhydrol.2010.02.022.

19 Dang, X.Z., Gao, M.S., Wen, Z., Jakada, H., Hou, G.H., Liu, S., 2020. Evolutionary  
20 process of saline groundwater influenced by palaeo-seawater trapped in coastal  
21 deltas: A case study in Luanhe River Delta, China. *Estuarine, Coastal and Shelf*  
22 *Science*, 244, 106894, doi: 10.1016/j.ecss.2020.106894.

- 1 de Montety, V., Radakovitch, O., Vallet-Coulomb, C., et. al., 2008. Origin of  
2 groundwater salinity and hydrogeochemical processes in a confined coastal  
3 aquifer: case of the Rhone delta (Southern France). *Applied Geochemistry*, 23(8),  
4 2337-2349, doi: 10.1016/j.apgeochem.2008.03.011.
- 5 Delsman, J. R., Huang, K. R. M., Vos, P. C., de Louw, P. G. B., Oude Essink, G. H. P.,  
6 Stuyfzand, P. J., and Bierkens, M. F. P., 2014. Paleo-modeling of coastal saltwater  
7 intrusion during the Holocene: an application to the Netherlands. *Hydrology and*  
8 *Earth System Sciences*, 18(10), 3891-3905, doi: 10.5194/hess-18-3891-2014.
- 9 Douglas, M., Clark, I.D., Raven, K., et al., 2000. Groundwater mixing dynamics at a  
10 Canadian Shield mine. *Journal of Hydrology*, 235, 88-103, doi: 10.1016/S0022-  
11 1694(00)00265-1.
- 12 Du, Y., Ma, T., Chen, L., et a., 2015. Genesis of salinized groundwater in Quaternary  
13 aquifer system of coastal plain, Laizhou Bay, China: Geochemical evidences,  
14 especially from bromine stable isotope. *Applied Geochemistry*, 2015, 59:155-165,  
15 doi: 10.1016/j.apgeochem.2015.04.017.
- 16 Du, Y., Ma, T., Chen L., et al., 2016. Chlorine isotopic constraint on contrastive genesis  
17 of representative coastal and inland shallow brine in China, *Journal of*  
18 *Geochemical Exploration*, 170 (2016): 21-29, doi: 10.1016/j.gexplo.2016.07.024.
- 19 Edmunds, W. M., 2001. Palaeowaters in European coastal aquifers-the goals and main  
20 conclusions of the PALAEAUX project, *Geological Society London Special*  
21 *Publications*, 189, 1-16, doi: 10.1144/GSL.SP.2001.189.01.02.
- 22 Fairbanks, R.G., 1989. A 17,000-year glacio-eustatic sea level record: influence of

- 1 glacial melting rates on the Younger Dryas event and deep ocean circulation.  
2 Nature, 342, 637-647, doi: 10.1038/342637a0.
- 3 Feng, J. and Zhang, W., 1998. The evolution of the modern Luanhe River delta, north  
4 China. *Geomorphology*, 25 (3), 269-278, doi: 10.1016/S0169-555X(98)00066-X.
- 5 Ferguson, G. and Gleeson, T., 2012. Vulnerability of coastal aquifers to groundwater  
6 use and climate change. *Nature Climate Change*, 2, 342-345, doi:  
7 10.1038/nclimate1413.
- 8 Fontes, J.C. and Matray, J.M., 1993. Geochemistry and origin of formation brines from  
9 the Paris Basin, France. 1. Brines associated with Triassic salts. *Chemical Geology*,  
10 109, 149-175, doi: 10.1016/0009-2541(93)90068-T.
- 11 Gao, S.M., 1981. Facies and sedimentary model of the Luan River delta. *Acta*  
12 *Geographica Sinica*, 48 (3), 303-314, doi: 10.11821/xb198103006 (in Chinese  
13 with English abstract).
- 14 Geriessh, M. H., Balke, K.-D., El-Rayes, A. E., and Mansour, B. M., 2015. Implications  
15 of climate change on the groundwater flow regime and geochemistry of the Nile  
16 Delta, Egypt, *Journal of Coastal Conservation*, 19, 589-608, doi: 10.1007/s11852-  
17 015-0409-5.
- 18 Giambastiani, B.M.S., Colombani, N., Mastrocicco, M., Fidelibus, M.D., 2013.  
19 Characterization of the lowland coastal aquifer of Comacchio (Ferrara, Italy):  
20 Hydrology, hydrochemistry and evolution of the system. *Journal of Hydrology*,  
21 501: 35-44, doi: 10.1016/j.jhydrol.2013.07.037.
- 22 Gibson, J.J., Edwards, T.W., Bursey, G.G., Prowse, T.D., 1993. Estimating evaporation

1 using stable isotopes: quantitative results and sensitivity analysis for two  
2 catchments in Northern Canada. *Nordic Hydrology*. 24, 79-94, doi:  
3 10.2166/nh.1993.0015.

4 Groen, J., Velstra, J., Meesters, A., 2000. Salinization processes in paleowaters in  
5 coastal sediments of Suriname: evidence from  $\delta^{37}\text{Cl}$  analysis and diffusion  
6 modelling. *Journal of Hydrology*, 234, 1-20, doi: 10.1016/S0022-1694 (00)00235-  
7 3.

8 Han, D.M., Kohfahl, C., Song, X.F., et al., 2011. Geochemical and isotopic evidence  
9 for Palaeo-Seawater intrusion into the south coast aquifer of Laizhou Bay, China.  
10 *Applied Geochemistry* 26 (5), 863-883, doi: 10.1016/j.apgeochem.2011.02.007.

11 Han, D. M., Song, X. F., Currell, M. J., et al., 2014. Chemical and isotopic constraints  
12 on the evolution of groundwater salinization in the coastal plain aquifer of Laizhou  
13 Bay, China, *Journal of Hydrology*, 508, 12–27, doi: /10.1016/j.jhydrol.  
14 2013.10.040.

15 Han, D.M., Currell, M.J., 2018. Delineating multiple salinization processes in a coastal  
16 plain aquifer, northern China: hydrochemical and isotopic evidence. *Hydrology  
17 and Earth System Science*, 22, 3473-3491, doi: 10.5194/hess-22-3473-2018.

18 Han, D.M., Cao G.L., Currell, M.J., et al., 2020. Groundwater salinization and flushing  
19 during glacial-interglacial cycles: insights from aquitard porewater tracer profiles  
20 in the North China Plain, China. *Water Resource Research*, 56 (11), doi:  
21 10.1029/2020WR027879.

22 He L., Amorosi A., Ye S.Y., et al., 2020. River avulsions and sedimentary evolution of

1 the Luanhe fan-delta system (North China) since the late Pleistocene. *Marine*  
2 *Geology*, 425,106194, doi: 10.1016/j.margeo.2020.106194.

3 Hendry, M.J. and Wassenaar, L.I., 2000. Controls on the distribution of major ions in  
4 pore waters of thick surficial aquitard. *Water Resources Research*, 36 (2), 503-513,  
5 doi: 10.1029/1999WR900310.

6 IAEA/WMO, 2006. Global Network of Isotopes in Precipitation, The GNIP Database,  
7 Vienna, available at: [http://www-naweb.iaea.org/napc/ih/IHS\\_resources\\_gnip.](http://www-naweb.iaea.org/napc/ih/IHS_resources_gnip.html)  
8 [html](http://www-naweb.iaea.org/napc/ih/IHS_resources_gnip.html).

9 Jiao, J.J. and Post, V., 2019. *Coastal Hydrology*. Cambridge University Press, New York.

10 Jin, X.F., 1984. The spore-pollen assemblages and the stratigraphy and  
11 palaeogeography in western Bohai Sea since late Pleistocene . *Marine Science*  
12 *Bullition* 3, 16-24, doi:  
13 CNKI:SUN:HYKX.0.1984-03-003 (in Chinese with English abstract).

14 Kooi, H., Groen, J., and Leijnse, A., 2000. Modes of seawater intrusion during  
15 transgressions, *Water Resource Research*, 36, 3581–3589, doi:  
16 10.1029/2000wr900243.

17 Kreuzer, A.M., Rohden, C.V., Friedrich, R., et al., 2009. A record of temperature and  
18 monsoon intensity over the past 40 kyr from groundwater in the North China Plain.  
19 *Chemical Geology*, 259, 168-180, doi: 10.1016/j.chemgeo.2008.11.001.

20 Larsen, F., Tran, L. V., Van Hoang, H., et. al., 2017. Groundwater salinity influenced by  
21 Holocene seawater trapped in incised valleys in the Red River delta. *Nature*  
22 *Geoscience*, 10, 376-381, doi: 10.1038/ngeo2938.

- 1 Lee, S., Currell, M., and Cendon, D. I., 2016. Marine water from mid-Holocene sea  
2 level highstand trapped in a coastal aquifer: Evidence from groundwater isotopes,  
3 and environmental significance. *Science of the Total Environment*, 544, 995-1007,  
4 doi: 10.1016/j.scitotenv.2015.12.014.
- 5 Li, G.X., Li, P., Liu, Y., et al., 2014 Sedimentary system response to the global sea level  
6 change in the East China Seas since the last glacial maximum. *Earth-Science  
7 Reviews*, 139 (2014), 390-405, doi: 10.1016/j.earscirev.2014.09.007.
- 8 Li, H.M. and Wang, J.D., 1983. Palaeomagnetic study on drill core from northern Bohai  
9 coastal plain. *Geochimica*, 2, 196-204 (in Chinese with English abstract).
- 10 Li, J., Liang, X., Jin, M. G., et. al., 2013. Geochemical signature of aquitard pore water  
11 and its paleo-environment implications in Caofeidian Harbor, China. *Geochemical  
12 Journal*, 47, 37-50, doi: 10.2343/geochemj.2.0238.
- 13 Li, Y.F., Gao, S.M. and An, F.T., 1982. A preliminary study of the Quaternary marine  
14 strata and its paleogeographic significance in the Luanhe delta region.  
15 *Oceanologia et Limnologia Sinica*, 13 (5), 433-439, doi:  
16 CNKI:SUN:HYFZ.0.1982-05-005 (in Chinese with English abstract).
- 17 Liu, S., Tang, Z., Gao, M. et. al., 2017. Evolutionary process of saline-water intrusion  
18 in Holocene and Late Pleistocene groundwater in southern Laizhou Bay. *Science  
19 of the Total Environment*, 607-608, 586-599, doi: 10.1016/j.scitotenv.2017.06.262.
- 20 Ma, F. S., Wei, A. H., Deng, Q. H., et. al., 2014. Hydrochemical Characteristics and the  
21 Suitability of Groundwater in the Coastal Region of Tangshan, China. *Journal of  
22 Earth Science*, 26 (6), 1067-1075, doi: 10.1007/s12583-014-0492-9.

- 1 Martínez, M.L., Intralawan, A., Vázquez, G., et. al., 2007. The coasts of our world:  
2 Ecological, economic and social importance. *Ecological Economics*, 63 (2-3),  
3 254-272, doi: 10.1016/j.ecolecon.2006.10.022.
- 4 Niu, Z.X., Jiang X.W. and Hu, Y.Z., 2019. Characteristics and causes of hydrochemical  
5 evolution of deep groundwater in the Luanhe delta. *Hydrogeology and*  
6 *Engineering Geology*, 46 (01), 27-34, doi: 10.16030/j.cnki.issn.1000-3665.2019.  
7 01.04 (in Chinese with English abstract).
- 8 Parkhurst, D.L., Appelo, C.A.J., 2013: Description of input and examples for  
9 PHREEQC version 3-a computer program for speciation, batch-reaction, one-  
10 dimensional transport, and inverse geochemical calculations, U.S. Geological  
11 Survey Techniques and Methods, book 6, chap. A43, 497 pp., available only at  
12 <http://pubs.usgs.gov/tm/06/a43/>.
- 13 Peng, G., Jiao, W.Q., Li, D.M., Li, G.Y., 1981. Division and correlation of the late  
14 Quaternary stratigraphy and discussion on the recent tectonic movement in the  
15 region of the Luanhe River Delta. *Seismology and Geology*, 3, 31-36 (in Chinese  
16 with English abstract).
- 17 Pearson, F.J. and Hanshaw, B.B., 1970. Sources of dissolved carbonate species  
18 ingroundwater and their effects on carbon-14 dating. In: IAEA (Ed.), *Isotope*  
19 *Hydrology*, IAEA, Vienna.
- 20 Post, V. E. and Kooi, H., 2003. Rates of salinization by free convection in high-  
21 permeability sediments: insight from numerical modeling and application to Dutch  
22 coastal area. *Hydrogeology Journal*, 11, 549-559, doi: 10.1007/s10040-003-0271-



1           7.

2    Qi, H., Ma, C., He, Z., et al. Lithium and its isotopes as tracers of groundwater  
3           salinization, 2019. A study in the southern coastal plain of Laizhou Bay, China.  
4           Science of The Total Environment, 650:878-890, doi:  
5           10.1016/j.scitotenv.2018.09.122.

6    Reilly, T. E. and Goodman, A. S., 1985. Quantitative analysis of saltwater-freshwater  
7           relationships in groundwater systems-a historical perspective. Journal of  
8           Hydrology, 80, 125-160, doi: 10.1016/0022-1694(85)90078-2.

9    Sanford, W.E., 2010. Groundwater hydrology: Coastal flow. Nature Geoscience, 3, 671-  
10          672, doi: 10.1038/ngeo958.

11   Santucci, L., Carol, E., Kruse E., 2016. Identification of palaeo-seawater intrusion in  
12          groundwater using minor ions in a semi-confined aquifer of the Río de la Plata  
13          littoral (Argentina). Science of the Total Environment, 566-567, 1640-1648, doi:  
14          10.1016/j.scitotenv.2016.06.066.

15   Small, C. and Nicholls, R. J., 2003. A global analysis of human settlement in coastal  
16          zones. Journal of Coastal Research. 19, 584-599, doi: 10.2307/4299200.

17   Sola F., Vallejos A., Daniele L., Pulido-Bosch A., 2014. Identification of a Holocene  
18          aquifer-lagoon system using hydrogeochemical data. Quaternary Research,  
19          82,121-131, doi: 10.1016/j.yqres.2014.04.012.

20   Stumpp, C., Ekdal, A., Gonenc, I.E. et al., 2014. Hydrological dynamics of water  
21          sources in a Mediterranean lagoon. Hydrology and Earth System Sciences,  
22          18(12):4825-4837, doi: 10.5194/hess-18-4825-2014.

- 1 Tran, D.A., Tsujimura M., Vo L.P., Nguyen V.T., Kambuku D., Dang T.D., 2020.  
2 Hydrogeochemical characteristics of a multi-layered coastal aquifer system in the  
3 Mekong Delta, Vietnam. *Environmental Geochemistry and Health*, 42, 661-680,  
4 doi: 10.1007/s10653-019-00400-9.
- 5 UN Atlas, 2010. 44 Percent of us Live in Coastal Areas, available at:  
6 [http://coastalchallenges.com/2010/01/31/un-atlas-60-of-us-live-in-the-coastal-](http://coastalchallenges.com/2010/01/31/un-atlas-60-of-us-live-in-the-coastal-areas)  
7 [areas.](http://coastalchallenges.com/2010/01/31/un-atlas-60-of-us-live-in-the-coastal-areas)
- 8 Vallejos A., Sola F., Yechieli Y., Pulido Bosch A., 2018. Influence of the  
9 paleogeographic evolution on the groundwater salinity in a coastal aquifer. Cabo  
10 de Gata aquifer, SE Spain. *Journal of Hydrology*, 557,55-66, doi:  
11 10.1016/j.jhydrol.2017.12.027.
- 12 van Engelen J., Oude Essink, Gualbert H.P., Kooi H., Bierkens Marc F.P., 2018. On the  
13 origins of hypersaline groundwater in the Nile Delta aquifer. *Journal of Hydrology*,  
14 560, 301-317, doi: 10.1016/j.jhydrol.2018.03.029.
- 15 van Engelen J., Verkaik J., King J., Nofal E.R., Bierkens M.F.P., Oude Essink G.H.P.,  
16 2019. A three-dimensional palaeohydrogeological reconstruction of the  
17 groundwater salinity distribution in the Nile Delta Aquifer. *Hydrology and Earth*  
18 *System Sciences*, 23, 5175-5198, doi: 10.5194/hess-23-5175-2019.
- 19 Wang, P.X., Min, Q.B., Bian, Y.H. et. al., 1981. Strata of Quaternary transgressions in  
20 east China: A preliminary study. *Acta Geologica Sinica*, 1981 (01), 1-13 (in  
21 Chinese with English abstract).
- 22 Wang, Y. and Jiao, J.J., 2012. Origin of groundwater salinity and hydrogeochemical

1 processes in the confined Quaternary aquifer of the Pearl River Delta, China.  
2 Journal of Hydrology, 438-439, 112-124, doi: 10.1016/j.jhydrol.2012.03.008.

3 Wang, Y., Fu, G., Zhang, Y., 2010. River-sea interactive sedimentation and plain  
4 morphological evolution. Quaternary Science, 27, 674-689, doi:  
5 10.3321/j.issn:1001-7410.2007.05.009, 2007 (in Chinese with English abstract).

6 Werner, A. D.: A review of seawater intrusion and its management in Australia,  
7 Hydrogeology Journal, 18, 281-285, doi: 10.1007/s10040-009-0465-8.

8 Werner, A. D., Bakker, M., Post, V. E. A., Vandenbohede, A., Lu, C., Ataie-Ashtiani, B.,  
9 Simmons, C. T., and Barry, D. A., 2013. Seawater intrusion processes, investigation  
10 and management: Recent advances and future challenges. Advance in Water  
11 Resources., 51, 3-26, doi:10.1016/j.advwatres.2012.03.004.

12 Xu, Q.M., Yuan, G.B., Zhang, J.Q., et al., 2011. Stratigraphic division of the Late  
13 Quaternary strata along the coast of Bohai bay and its geology significance. Acta  
14 Geologica Sinica, 85 (8), 1352-1367, doi: CNKI:11-1951/P.20110804.1239.004  
15 (in Chinese with English abstract).

16 Xu, Q.M., Yang, J.L., Yuan, G.B., Chu, Z.X., Zhang, Z.K., 2015. Stratigraphic sequence  
17 and episodes of the ancient Huanghe Delta along the southwestern Bohai Bay  
18 since the LGM. Marine Geology, 367, 69-82, doi: 10.1016/j.margeo.2015.05.008.

19 Xu, Q.M., Yang, J.L., Hu, Y.Z., Yuan, G.B., Deng, C.L., 2018. Magnetostratigraphy of  
20 two deep boreholes in the southwestern Bohai Bay: its tectonic implications and  
21 constraints on ages of volcanic layers. Quaternary Geochronology, 43, 102-114,  
22 doi: 10.1016/j.quageo.2017.08.006.

- 1 Xu, Q.M., Meng, L.S., Yuan, G.B., et al., 2020. Transgressive wave-and tide-dominated  
2 barrier-lagoon system and sea-level rise since 8.2 ka recorded in sediments in  
3 northern Bohai Bay, China. *Geomorphology* 352, 106978, doi:  
4 10.1016/j.geomorph.2019.106978.
- 5 Xue, C.T., 2009. Historical changes of coastlines on west and south coasts of Bohai Sea  
6 since 7000 a B.P. *Scientia Geographica Sinica*, 29, 217-222, doi:  
7 10.3969/j.issn.1000-0690.2009.02.012 (in Chinese with English abstract).
- 8 Xue, C.T., 2014. Missing evidence for stepwise postglacial sea level rise and an  
9 approach to more precise determination of former sea levels on East China Sea  
10 Shelf. *Marine Geology*, 348, 52-62, doi: 10.1016/j.margeo.2013.12.004.
- 11 Xue, C.T., 2016. Extents, type and evolution of Luanhe River fan-delta system, China.  
12 *Marine Geology & Quaternary Geology*, 36 (06), 13-22, doi:  
13 CNKI:SUN:HYDZ.0.2016-06-004 (in Chinese with English abstract).
- 14 Zhou, X., 2013. Basic characteristics and resource classification of subsurface brines in  
15 deep-seated aquifers. *Hydrogeology & Engineering Geology*, 40 (5), 4-10, doi:  
16 CNKI:SUN:SWDG.0.2013-05-004 (in Chinese with English abstract).